

Co-learning Planning and Control Policies Using Differentiable Formal Task Constraints

Zikang Xiong, Joe Eappen, Daniel Lawson, Ahmed H. Qureshi, and Suresh Jagannathan

Abstract—This paper presents a hierarchical reinforcement learning algorithm constrained by differentiable signal temporal logic. Previous work on logic-constrained reinforcement learning consider encoding these constraints with a reward function, constraining policy updates with a sample-based policy gradient. However, such techniques oftentimes tend to be inefficient because of the significant number of samples required to obtain accurate policy gradients. In this paper, instead of implicitly constraining policy search with sample-based policy gradients, we directly constrain policy search by backpropagating through formal constraints, enabling training hierarchical policies with substantially fewer training samples. The use of hierarchical policies is recognized as a crucial component of reinforcement learning with task constraints. We show that we can stably constrain policy updates, thus enabling different levels of the policy to be learned simultaneously, yielding superior performance compared with training them separately. Experiment results on several simulated high-dimensional robot dynamics and a real-world differential drive robot (TurtleBot3) demonstrate the effectiveness of our approach on five different types of task constraints. Demo videos, code, and models can be found at our project website: <https://sites.google.com/view/dsrl>.

I. INTRODUCTION

Logic-Constrained Reinforcement Learning (LCRL) [1], [2], [3], [4], [5], [6], [7], [8], [9], [10], [11] is a rapidly growing field that enables end-to-end reinforcement learning to perform various high-level tasks. For example, a logical task constraint can require a drone to hover near a doorway around until the door is opened, execute a collection of complex instructions sequentially, or make decisions that are tailored to different conditions. However, there exists a sizable representation and conceptual gap between the behaviors expressible by symbolic logical constraints and those that are admitted by policy parameters that govern the behaviors of a Deep Reinforcement Learning (DRL) system. To bridge this divide, prior work has enriched symbolic constraints with quantitative semantics such as Signal Temporal Logic (STL) [2], [12]. In this setting, logical specifications serve primarily to help generate the reward function used by a DRL procedure; this approach is known as reward shaping. However, as we show in this paper, by equipping these enriched semantics with differentiable operators [13], [14], policy updates can be meaningfully constrained to yield a significantly more sample-efficient learning technique compared with existing reward-shaping methods.

Constrained reinforcement learning [15], [16], [17] is a fundamental technique used in DRL implementations. Con-

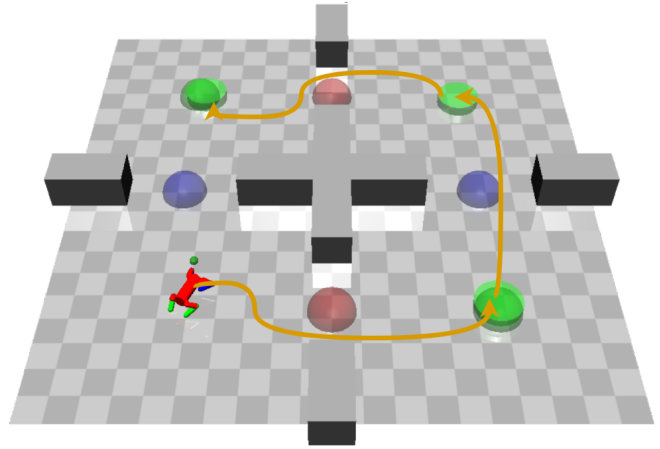


Fig. 1: Branch task. Upon visiting a waypoint of a specific color, the *Doggo* robot must visit the other waypoint with the same color. The green cylinders serve as intermediate goals for the low-level goal-conditioned control policy, which is guided by the learned residual planning policy. The orange control trajectory produced by the control policy satisfies the task constraints by visiting both green waypoints.

straints can vary for the different algorithms; for example, CPO [17] learns a safety surrogate function as a constraint, while PPO [16] and TRPO [15] constrain the KL-divergence between the old and new policy. Perhaps the most widely-used technique incorporating these constraints is the Lagrangian method. Because solving the Lagrangian equation with dual gradient descent (e.g., [17], [18]) requires that the constraints must be differentiable, differentiable formal constraints [13], [14] provide a natural means of integrating formal constraints within a constrained reinforcement learning pipeline. However, unlike CPO [17] that learns surrogate safety constraints, and PPO [16] and TRPO [15] that only bound KL-divergence, in this paper, we explore how differentiable formal constraints provide the ability to program various tasks and realize their solutions within a hierarchical reinforcement learning framework.

Hierarchical policies have proven to be effective in complex tasks [9], [19], [20], [21]. For example, it is quite common to use a high-level planning policy to guide low-level control policies [21], [22]. While part of the effectiveness of such approaches comes from the decomposition of tasks, an important by-product of such decompositions is that it allows different levels in the hierarchy to learn jointly, adapting to each other as necessary, thereby improving policy

Authors affiliate to Computer Science Department, Purdue University, IN 47906, USA. (E-mail: xiong84@purdue.edu; jeappen@purdue.edu; lawson95@purdue.edu; ahqureshi@purdue.edu; suresh@cs.purdue.edu)

performance.

In this work, a high-level residual planning policy, constrained by a formal specification, provides a sequence of goals to guide a low-level goal-conditioned control policy to satisfy this specification. Additionally, our experimental results demonstrate that joint training is typically necessary because a high-level planner often needs to know the capabilities of the low-level controller to generate a correct plan, and a low-level controller can learn to adapt its behaviors to the specific plan generated by the planner for better performance. Our contributions are as follows:

- We integrate differentiable task constraints into a constrained reinforcement learning framework, yielding a sample-efficient algorithm effective across a range of problems with high-dimensional continuous dynamics, which outperforms previous LCRL work based on reward shaping.
- We show that differentiable formal specifications can stably constrain a hierarchical policy, and enable co-learning between different policy levels, resulting in superior performance when compared to training each level separately.
- We justify our design choices with detailed experimental and ablation studies.

II. RELATED WORK

Integrating symbolic techniques with deep learning has led to recent interest in different learning domains [23]. In this work, we consider symbolic constraints written in Linear Temporal Logic (LTL) [24] and its quantitative semantics STL [12]. LTL is widely used in specifying various planning and control tasks [25], [26], [27], [28]. Along with the advances in reinforcement learning in an unknown, stochastic environment, a line of work [1], [2], [3], [4], [5], [21], [6], [7], [8], [9], [10] has considered how to combine LTL-specified tasks with reinforcement learning. However, these approaches formulate such an integration as either continuous or discrete rewards, and optimize policies with sample-based policy gradients, leading to sample-inefficient or even intractable algorithms [29].

Lagrangian-based constrained reinforcement learning [15], [17], [16] provides another perspective to enforce constraints on policies. Given a differentiable constraint, these methods can enforce constraints only on the policy without reward shaping. However, this prior work has not considered how to synergistically take advantage of policies with differentiable [13], [14] and programmable [30], [31], [32] formal constraints whose definitions can directly encode the high-level tasks. More recently, a constrained reinforcement learning framework with formal constraints [11] was proposed and provided a theoretical foundation for constrained reinforcement learning under formal constraints in a discrete state and action space. However, this work does not consider directly backpropagating through formal constraints and requires learning high-level abstractions, making it perform modestly in the high-dimensional continuous control tasks we consider.

Our work also relates to gradient-based motion planning [13], [14], [33], [34], [35]. While they are typically only applicable when the dynamics are known and deterministic, our focus is on planning in the face of unknown and stochastic dynamics. Lastly, our high-level planning policy is related to planning networks [36]. However, learning a planning neural network in a DRL loop under task constraints, which benefits both the planning policy and control policy, has not been explored previously.

III. BACKGROUND

a) Lagrangian Method with Dual Gradient Descent:

The Lagrangian method solves constrained optimization problems. For a real vector \mathbf{x} , consider the equality-constrained problem:

$$\max_{\mathbf{x}} f(\mathbf{x}) \quad \text{s.t. } h(\mathbf{x}) = 0,$$

where $h(x)$ is the constraint function and the $f(x)$ is the objective function. This can be expressed as a problem with the Lagrange multiplier λ . Let $\mathcal{L}(\mathbf{x}, \lambda) = f(\mathbf{x}) + \lambda h(\mathbf{x})$,

$$(\mathbf{x}^*, \lambda^*) = \arg \min_{\lambda} \max_{\mathbf{x}} \mathcal{L}(\mathbf{x}, \lambda), \quad (1)$$

which can be solved by iteratively updating the primal variable \mathbf{x} and dual variable λ with gradients [18]. The λ here acts as “dynamic” penalty coefficients for updating on real vector \mathbf{x} . Lagrangian methods are widely used in the policy gradient update of many popular constrained DRL algorithms [16], [17]. Note that to compute the gradient through the constraint function $h(\mathbf{x})$, the function h must be differentiable. Since we want to constrain training with formal constraints, we, therefore, introduce differentiable STL [12], [14] below.

b) *Differentiable Signal Temporal Logic*: The syntax of STL contains both first-order logic operators \wedge (and), \neg (not), \vee (or), \Rightarrow (implies), and temporal operators \bigcirc (next), $\diamond_{[a,b]}$ (eventually), $\square_{[a,b]}$ (globally), $\mathcal{U}_{[a,b]}$ (until). The initial time a and end time b “truncate” a path. For example, $\square_{[a,b]}$ qualifies property that globally holds during time a and b . The syntax of STL is recursively defined via the following grammar:

$$\begin{aligned} \phi := & \top \mid \perp \mid \mathcal{P} \mid \neg\phi \mid \phi \wedge \psi \mid \phi \vee \psi \mid \phi \Rightarrow \psi \\ & \mid \bigcirc\phi \mid \diamond_{[a,b]}\phi \mid \square_{[a,b]}\phi \mid \phi \mathcal{U}_{[a,b]}\psi, \end{aligned} \quad (2)$$

where $\mathcal{P} : \mathbb{R}^n \rightarrow \mathbb{R}$ is a predicate function mapping a state to a real value. Like [13], [14], all the predicates here are differentiable functions. With this syntax, for example, the branch task in Fig. 1 can be written as

$$\bigvee_{i=1}^{\frac{N}{2}} \left(\diamond_{[1,T]}\phi_i \wedge \square_{[1,T]} \left(\phi_i \Rightarrow \diamond_{[t,T]}\phi_{2i} \right) \right), \quad (3)$$

where N is even. The ϕ_i and ϕ_{2i} are predicates that specify waypoints with the same color. This specification defines that a robot must visit any waypoint specified by ϕ_i , and it will visit the other one with the same color (specified by ϕ_{2i}) eventually.

The quantitative semantics of STL represent symbolic constraints using predicates, min, and max operators in the numeric space. Readers can refer to [12], [13], [14] and our project website for the complete quantitative semantics. [13], [14] have demonstrated how to backpropagate through these logic structures. [13], [14] also suggest that min and max operators can be smoothed with *softmin* and *softmax* functions to achieve smooth gradients. We further provide empirical discussion for the smooth min and max in Sec. V-D.

IV. APPROACH

The overview of our approach, Differentiable Specification Constrained Reinforcement Learning (DSCRL), is provided in Fig. 2.

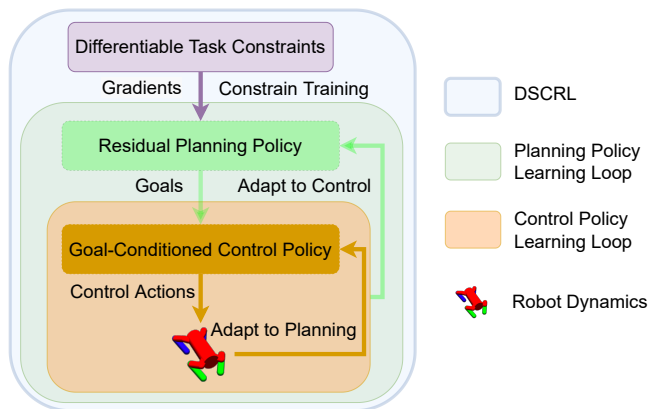


Fig. 2: Hierarchical structure of DSCRL. Differentiable STL allows users to define task constraints that restrict residual planning updates. The planning policy generates subgoals to guide a low-level control policy, helping to achieve the task. During training, the goal-conditioned control policy learns to reach subgoals by maximizing a control reward. The planning policy receives feedback from the control reward and refines its subgoals while considering task constraints.

A. Residual Planning Policy

a) *Planning Network Structure*: The high-level policy in DSCRL is a residual planning network of the form shown in Fig. 3. This network predicts the *deviation* between subgoals (i.e., g_i in Fig. 3) with a Gated Recurrent Unit (GRU). We choose this structure for three reasons. Firstly, STL planning tasks require memory of past states, as seen in the *Branch* task (Fig. 1), where a planning policy needs to recall the previous waypoint visited to decide the next waypoint that should be reached. This memory is provided by the GRU. Secondly, residual connections aid backpropagation in long-planned paths [37], [38]. Thirdly, this structure generates the next subgoal by adding the predicted deviation to the current subgoal, allowing us to limit the distance between neighbor subgoals with an upper bound on deviation (e.g., with a scaled *tanh*), making them more realistic for the low-level control policy to follow.

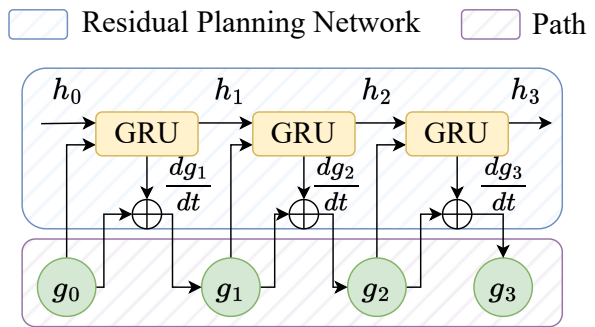


Fig. 3: Residual Planning Network. The key difference between this network structure and a recurrent network is that our GRU predicts the deviation (a.k.a. residual [37], [38]) between subgoals, instead of directly predicting subgoals, which eases gradient backpropagation for long sequences.

b) *Stochastic Planning Policy*: The high-level policy π_θ^h is a stochastic planning network parameterized by θ . Stochasticity can be easily introduced by adding a distribution layer on the GRU cell and sampling $\frac{dg_i}{dt}$ from the distribution. Backpropagation through the distribution layer can be handled by a reparameterization trick [39]. We train the planning network to maximize the objective function:

$$\mathcal{L}(\theta, \lambda) = \mathbb{E}_{\tau \sim \pi_\theta^h} \left(\pi_\theta^h(\tau) r^h(\tau) + \lambda(\epsilon - \rho(\tau, \phi)) \right). \quad (4)$$

$\pi_\theta^h(\tau)$ returns the probability of a path τ under policy π_θ^h . Notably, $r^h(\tau) = \sum_{i=0}^T r_t^l$ is the cumulative *control* reward (Sec. IV-B). Maximizing $\pi_\theta^h(\tau) r^h(\tau)$ will maximize the expected cumulative control rewards when following paths sampled from π_θ^h , which adapts the high-level planning policy to the low-level control policy. $\lambda(\epsilon - \rho(\tau, \phi))$ is the Lagrangian term. $\rho(\tau, \phi)$ evaluates the path τ with a STL formula ϕ , and returns a quantitative value. To ensure that constraint ϕ is satisfied (i.e., $\rho(\tau, \phi) > 0$), we introduce a small positive ϵ . When the gradient optimization algorithm keeps $\epsilon - \rho(\tau, \phi)$ close to zero, $\rho(\tau, \phi) > 0$ is guaranteed.

We update the high-level policy parameters θ with the constrained gradient in an *ascent* direction corresponding to the max operator in Eq. (1):

$$\nabla_\theta \mathcal{L}(\theta, \lambda) = \mathbb{E}_{\tau \sim \pi_\theta^h} \left(\nabla_\theta \log \pi_\theta^h(\tau) r^h(\tau) - \lambda \nabla_\theta \rho(\tau, \phi) \right) \quad (5)$$

Here, we can compute $\nabla_\theta \rho(\tau, \phi)$ because τ is sampled from π_θ^h and the STL semantics ρ is differentiable. After updating the primal variable θ , we update the dual variable λ with the gradient in the *descent* direction corresponding to the min operator in Eq. (1):

$$\nabla_\lambda \mathcal{L}(\theta, \lambda) = \epsilon - \rho(\tau, \phi). \quad (6)$$

The reward $r^h(\tau)$ is a cumulative control reward r_t^l when following path τ . A larger $r^h(\tau)$ indicates that the generated path is easier to follow (e.g., a short path without collision) by the low-level control policy, while a larger $\rho(\tau, \phi)$

indicates that the specification is more “robust” to satisfy. By optimizing Eq. (4), the planning policy considers the capability of the low-level control policy and simultaneously satisfies the constraints.

B. Goal-Conditioned Control Policy

The low-level control policy $\pi^l(o_t | g)$ is a goal-conditioned policy [40] trained with PPO [16], where g is sampled from the high-level policy π^h , and o_t is the robot observation at time t . The control reward r_t^l is defined as

$$r_t^l = \|g - x_{t-1}\|_2 - \|g - x_t\|_2, \quad (7)$$

where x_t is the position of the robot at time t . The reward is positive if and only if the robot gets closer to the planned goal g . Because g is sampled from π^h , the control policy is optimized for a smaller goal space, also making it specialized to the high-level policy.

C. DSCRL Co-learning Algorithm

Algorithm 1: DSCRL

```

1 def Rollout( $n$ : int)  $\rightarrow$  Buffer:
2   for  $j = 1, 2, \dots, n$  do
3      $g_0 = \text{SampleInitial}()$ ;
4      $\tau = \text{ForwardPath}(\pi^h, g_0)$ ;
5      $[o], [r^l] = \text{Simulation}(\pi^l, \tau)$ ;
6      $\mathcal{B}.add(\tau, [o], [r^l])$ ;
7   return  $\mathcal{B}$ ;

8 for  $i = 1, 2, \dots, N$  do
9   for  $i = 1, 2, \dots, N^h$  do
10    High-level Buffer  $\mathcal{B}^h \leftarrow \text{Rollout}(n^h)$ ;
11    UpdatePlan( $\phi, \pi^h, \mathcal{B}^h$ ); // Sec. IV-A
12  for  $i = 1, 2, \dots, N^l$  do
13    Low-level Buffer  $\mathcal{B}^l \leftarrow \text{Rollout}(n^l)$ ;
14    UpdateCtrl( $\pi^h, \pi^l, \mathcal{B}^l$ ); // Sec. IV-B

```

Algorithm 1 displays the full structure of the DSCRL algorithm for a specification ϕ . Lines 1 to 7 define rollout function sampling paths, observations, and control rewards. The sampled data will be stored in a buffer \mathcal{B} . Line 3 randomly samples an initial position g_0 , and line 4 does a forward sampling with this initial position to generate a path τ . Random initialization during training gives the trained residual planning policies the ability to plan from random initial positions. Line 5 collects the observations and control rewards with the planned path τ and control policy π^l .

Lines 8 to 14 perform hierarchical updates for the planning and control policies. These policies are updated with different buffers for stability purposes [41]. Line 10 encapsulates the discussion given in Sec. IV-A where the differentiable constraint ϕ enforces the planning policy to achieve high-level tasks while also maximizing control rewards by placing “control-friendly” subgoals. Line 14 corresponds encapsulates the discussion given in Sec. IV-B, where the control

policy is trained to follow and adapt the paths provided by the planning policy.

V. EXPERIMENTS

A. Environments and Specifications

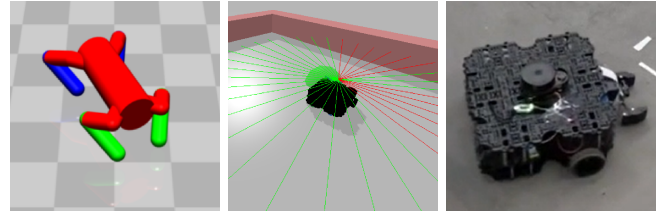


Fig. 4: From left to right: A simulated *Doggo*, a simulated *TurtleBot3*, and a real *TurtleBot3*. The control policy for *Doggo* utilizes 58-dimensional observation space including IMU and position data and 4-dimensional action space consisting of 8 hip and 4 ankle control commands. Meanwhile, the control policy for the *TurtleBot3* is based on 4-dimensional IMU data and 36-dimensional down-sampled LiDAR data for obstacle distance measurement. Its action space contains the control commands of the two wheels. More simulated environments are provided on our website.

a) *Environments*: We evaluate our training algorithm on a range of simulation environments and deployed trained policies to a real-world *TurtleBot3*. The simulation dynamics are collected from Safety-Gym [42] and PyBullet [43], [44]; full demonstrations for these environments are provided on our website. We present the results of the most difficult *Doggo* simulation in this suite and both the simulated and real *TurtleBot3*. The policies deployed on the real *TurtleBot3* are trained in simulation.

b) *Specifications*: We consider five types of specifications. They are *Sequence*, *Cover*, *Branch*, *Loop*, and *Signal*. *Sequence* tasks require a robot to reach goals in a given order. In contrast, the *Cover* tasks only require a robot to reach all goals without considering the order in which they are visited. *Branch* tasks are defined in terms of conditional behaviors. For example, *if visiting A then also visit B; if visiting C then also visit D*, etc. *Loop* tasks require robots to repeatedly visit a set of goals, while *Signal* tasks require robots to repeatedly visit a set of goals until a certain condition is satisfied. The *Branch* task of *Doggo* robot is shown in Fig. 1. In Fig. 5, we visualize the *Sequence*, *Cover*, *Loop*, and *Signal* tasks and provide their formal STL specifications for the *Doggo* robot.

B. Sample-Efficient Logical-Constrained Training

We first compare DSCRL with previous approaches in terms of end-to-end training sample complexity. One significant difference between DSCRL and previous logical-constrained reinforcement learning algorithms is that we are able to directly differentiate through constraints, while prior work estimate policy gradients from the sample and shaped rewards [1], [2], [3], [4], [5], [6], [7], [8], [9], [10]. These reward shaping approaches can be divided into two categories. [2], [6], [10] shape the reward with quantitative rules (e.g.,

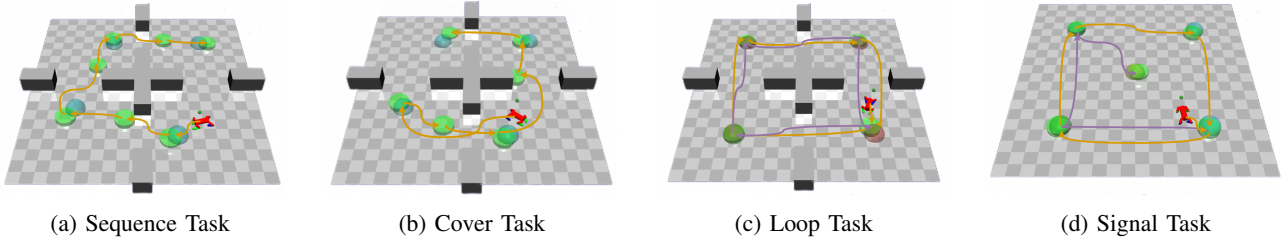


Fig. 5: *Doggo* executes *Sequence*, *Cover*, *Loop*, and *Signal* tasks. The *Sequence* task ($\bigwedge_{i=0}^N \diamond_{[t_i, t_{i+1}-1]} \phi_i$) ensures that all goals are reached in order (Fig.5a). The *Cover* task ($\bigwedge_{i=0}^N \diamond_{[1, T]} \phi_i$) ensures that all waypoints are eventually reached in an arbitrary order (Fig.5b). The *Loop* task ($\square_{[1, T]} \left(\bigvee_{i=0}^N \phi_i \wedge \bigwedge_{i=0}^N (\phi_i \Rightarrow \bigcirc \phi_{(i+1) \bmod N}) \right)$) ensures that the robot visits a series of waypoints in a specific order, while looping among them (Fig.5c). The *Signal* task ($\diamond_{[1, T]} \phi_{N+2} \wedge \left(\bigvee_{i=0}^N \phi_i \wedge \bigwedge_{i=0}^N (\phi_i \Rightarrow \neg \bigcirc \phi_i) \right) \mathcal{U}_{[1, T]} \phi_{N+1}$) is a loop with an exit condition (ϕ_{N+1}). In Fig. 5d, the robot exits the loop at the second waypoint in the second loop and eventually reaches the center waypoint specified by ϕ_{N+2} .

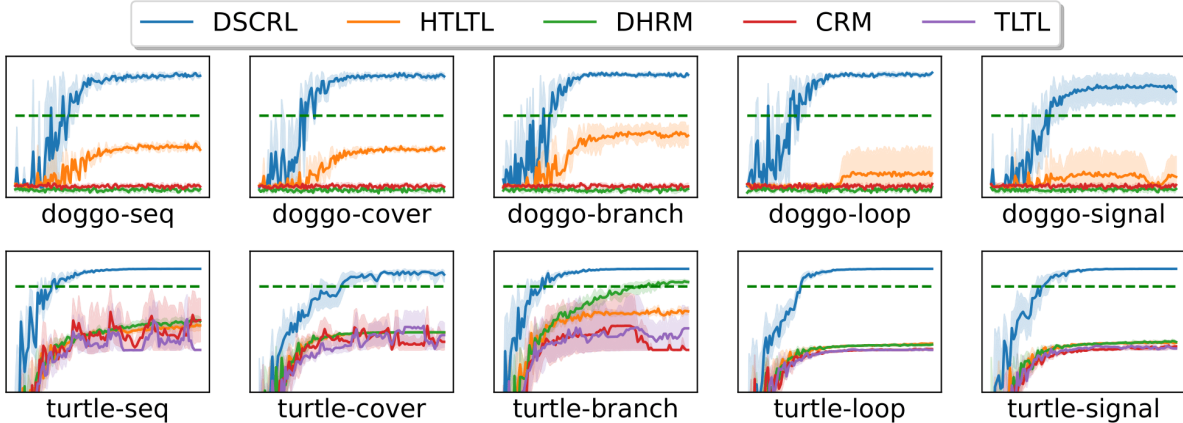


Fig. 6: Specification scores (y-axis) against the simulation steps (x-axis) during training. A higher score means that the generated control trajectory was more robust to achieving a task (e.g., closer to the waypoints it should arrive). When the curve is above the green dashed line, the task specification is satisfied (e.g., in a *Sequence* task, the generated path gets close enough to all the goals in order). We trained every algorithm with 5 different random seeds. The complete steps for *Doggo* are 1×10^8 , and 1×10^6 for the simulated *TurtleBot3*. The tasks from left to right are *Sequence*, *Cover*, *Branch*, *Loop*, and *Signal*, respectively

STL), while [1], [3], [4], [5], [8], [7], [9] first turn logical constraints into automata, and define reward functions over these structures. We compare our algorithm with TLTL [2], CRM [9], and DHRM [9] as representatives of these different types of approaches. HTLTL is a hierarchical version of TLTL, the STL score and cumulative control reward is used to train a high-level policy, while training the low-level policy follows the same approach introduced in Sec. IV-B.

Fig. 6 supports our hypothesis that DSCRL can converge to satisfiable scores with fewer simulation steps (i.e., samples). In all the *Doggo* tasks with challenging control dynamics, only the HTLTL algorithm was able to make progress, while all the other algorithms are unable to make meaningful anything in the same amount of simulation steps. On the simulated *TurtleBot3*, our results also show the hardness of learning feasible planning policies with reward shaping. Except for the DHRM on *Branch* task, almost all the reward-shaping algorithms cannot reach a decent score in given simulation steps.

In Table I, we fixed the training of control policies,

TABLE I: Number of gradient updates in only training a planning network with over 95% success rate. We perform each experiment five times with the number of successful runs given in parentheses.

Tasks	Reward Shaping	DSCRL
<i>Sequence</i>	9866 \pm 0 (1)	641 \pm 102 (5)
<i>Cover</i>	N/A (0)	783 \pm 584 (5)
<i>Branch</i>	9721 \pm 210 (2)	722 \pm 527 (5)
<i>Loop</i>	N/A (0)	1247 \pm 150 (5)
<i>Signal</i>	N/A (0)	1509 \pm 420 (5)

and further compare the training efficacy of a high-level planning policy using a policy gradient and differentiable constraint methods. Reward-shaping algorithms estimate the logic-constrained policy gradient with samples, while DSCRL backpropagates directly through the differentiable constraints, providing accurate gradients without extensive sampling. For each of the five tasks, we perform five experiments with the reward-shaping method using 100 trajec-

TABLE II: Jointly v.s. Separately Training

Metrics	Satisfaction Rate \uparrow					Time to Finish (in sec.) \downarrow				
	Tasks	Sequence	Cover	Branch	Loop	Signal	Sequence	Cover	Branch	Loop
<i>Doggo</i>	0.98 /0.30	0.96 /0.28	0.97 /0.88	0.95 /0.64	0.97 /0.63	46.29 /64.64	56.99 /73.71	44.57 /56.37	150.33 /170.46	157.11 /172.03
<i>Turtlebot3</i> (Simu)	0.99 /0.21	0.98 /0.37	0.99 /0.43	0.93 /0.23	0.95 /0.31	34.23 /45.18	31.97 /43.53	13.62 /35.29	130.27 /172.12	85.91 /102.10
<i>Turtlebot3</i> (Real)	1.0 /0.0	1.0 /0.33	1.0 /0.33	1.0 /0.0	1.0 /0.33	35.33 /NA	32.67 /42.00	14.67 /24.00	133.67 /NA	84.33 /95.00

ries to estimate the policy gradients, and the differentiable constraint method using 100 sampled initial positions to compute gradients for each update. We stop training after 95 of the 100 trajectories in a batch satisfy the corresponding constraint.

In each column of Table I, the number before and after \pm is the mean and standard deviation of gradient updates, respectively. N/A means in 5 runs, the algorithm failed to train a planning policy with over 95% satisfaction rate in 10000 gradient updates. The number in the parentheses for each task is the total number (out of 5) of successful runs. For all the five tasks evaluated, our differentiable constraint approach results in at least $13.47\times$ fewer gradient steps and can always train a high-level planning policy with over 95% satisfaction rate with 1500 or fewer gradient updates. Reward shaping only succeeds once in *Sequence* and twice in *Branch*, requiring significantly more gradient updates (e.g., 9800 for *Sequence* and 9700 for *Branch*).

C. Joint Learning Under Constraints

DSCRL takes task constraints into consideration while enabling joint learning across different levels. This type of joint learning is essential for most tasks, as it allows the high-level planner to leverage the low-level controller’s capabilities to create an effective plan. Similarly, the low-level controller can adapt to the specific high-level plan to achieve better performance. This distinguishes our hierarchical learning algorithm from existing STL planning approaches, such as gradient-based planning [13] and Mixed-Integer Linear Programming (MILP) [45]. These approaches cannot jointly optimize both the planning and control policies, especially for high-dimensional unknown dynamics and neural network control policies that we consider.

a) Better Performance: To demonstrate the benefits of joint training, we compared policies trained with DSCRL to separately trained policies with the same network and algorithm structure, but that does not consider information that can be gleaned from the other level. The separately trained policies remove the term $\pi_{\theta}^h(\tau)r^h(\tau)$ in Eq.(4) and randomly sample the subgoal g during training of the goal-conditioned control policy described in Sec.IV-B.

Table II compares the performance of policies jointly trained by DSCRL (shown as data before /) and separately trained policies (shown as data after /) in terms of satisfaction rate and time to finish tasks. We evaluate the policies with 100 simulation runs for simulation tasks (*Doggo* and *TurtleBot3* (Simu)), and 3 runs for the real *TurtleBot3*. A task is considered satisfied if the robot generates a trajectory satisfying the task constraint within a given time limit of 200 seconds for *Doggo*, simulated and real *TurtleBot3*. The

jointly trained policies (bold) by DSCRL significantly and identically outperform the separately trained policies in all tasks.

b) A Failure Case without Joint Learning: Joint training lets each level consider the other level’s capabilities. Without such consideration, trained policies can easily produce unrealistic behaviors. For example, the planning policy may set a subgoal very far away from an existing position or even against a wall, and the control policy may never be able to guide the robot to reach this subgoal. Fig. 7 shows exactly such a case. A planner that does not account for the control

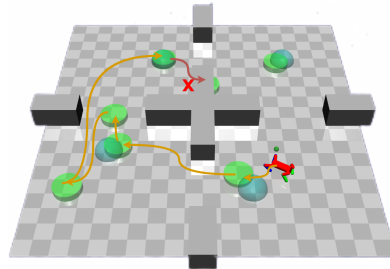


Fig. 7: Path generated by planner without adaptation to control policy. The robot is finally stuck at the place marked with the red cross.

policy can also generate a path satisfying the *Sequence* task constraint shown in Fig. 7 (i.e., reaching all the waypoints in order), but completely discard how the control policy can reach these waypoints. In contrast, the jointly trained planning policy generates an easy-to-follow path (shown in Fig. 5a) for the control policy.

D. More Ablations

a) Choice of Planning Network: Our planning policy is built upon a residual policy network (Fig. 3), which has benefits both in terms of gradient backpropagation and memory about the past. In Fig. 8, we show the results of an ablation study on the *Doggo* for all five tasks. These results confirm that the residual policy outperforms both Multilayer Perceptron (MLP) and standard GRU policies in almost every case. For example, on the *Sequence* task, the residual policy outperforms MLP and GRU by 65% and 51% resp. on the satisfaction rate and 29% and 18% resp. on the steps to reach.

b) Smooth STL: [13], [14] observe that smooth STL benefits gradient-based planning. However, we show that this may not always be the case when STL is part of a loss function (e.g., as a Lagrangian term). Intuitively, choosing smooth and non-smooth STL is analogous to choosing an L_2 or L_∞ loss (L_2 loss based on MSE is “smooth” while L_∞ loss based on max is “non-smooth”).

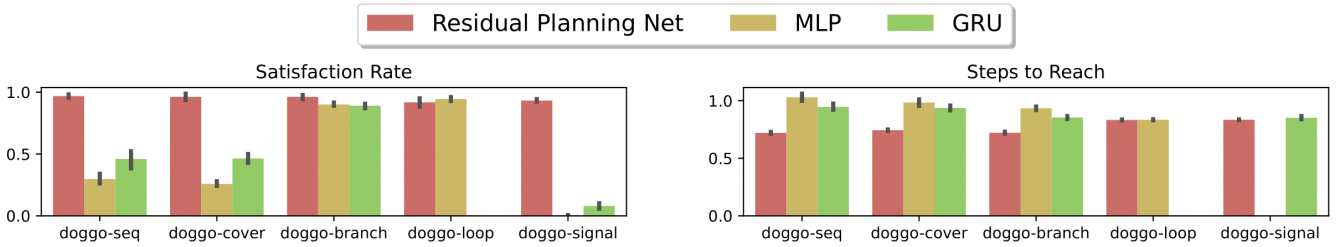


Fig. 8: Planning Network Ablation. The GRU policy on *Loop* task and the MLP policy on *Signal* task failed to reach all the time, so their data is absent from the plot.

We conducted an ablation study showing the efficiency of smooth and non-smooth STL loss in terms of the number of gradient updates. We trained our planning policy network (without considering control policy) with both smooth and non-smooth STL loss, stopping training when the policy could generate 95% of paths satisfying the STL specification. Each cell in Table III is the result of 5 training runs. The mean and standard deviation are before and after \pm , resp. The results in Table III are mixed. Smooth STL loss performs significantly better on task *Sequence* and *Signal*, but slightly worse on the other tasks on average.

TABLE III: Number of gradient updates required for satisfactory performance in smooth vs non-smooth STL constraints

Tasks	Smooth STL	Non-Smooth STL
<i>Sequence</i>	268.20 \pm 80.45	710.20 \pm 193.76
<i>Cover</i>	1090.60 \pm 428.56	1035.00 \pm 370.58
<i>Branch</i>	49.00 \pm 24.23	43.20 \pm 9.74
<i>Loop</i>	119.20 \pm 23.07	112.60 \pm 35.57
<i>Signal</i>	352.40 \pm 289.79	588.00 \pm 128.79

c) *Advantage in Planning Time:* Except for the benefits of joint learning mentioned in V-C, our trained policy can also plan faster than MILP- and gradient-based planning.

TABLE IV: Planning time (in sec.) comparison

Tasks	Planning Policy	MILP	Gradient
<i>Sequence</i>	0.0017	0.0961	0.8428
<i>Cover</i>	0.0017	0.2185	3.4847
<i>Branch</i>	0.0014	0.0789	7.2043
<i>Loop</i>	0.0048	7.4238	10.4809
<i>Signal</i>	0.0024	7.8531	2.6706

Table IV reports the planning time comparison. The planning policy is a neural network that generates planning paths from randomly sampled initial states. A forward propagation in milliseconds will produce a path, that will take MILP [45] or gradient techniques [14], [13] several seconds to solve. We quantify the planning time in Table IV, which is the average time (in sec.) over 100 runs. Our planning policy is at least $55\times$ faster than MILP planners and $489\times$ faster than gradient-based planners.

E. Extension with Neural Predicate

Lastly, we note that our algorithm can be combined with any differentiable predicate, such as Neural Signed

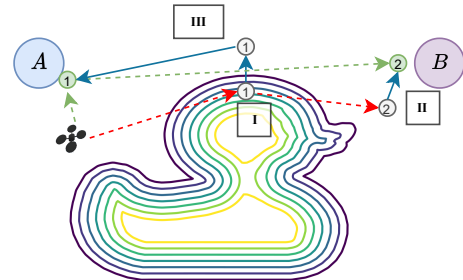


Fig. 9: A task requires covering waypoints A and B while avoiding the duck obstacle specified by a neural SDF. Step I, II, and III show how the backpropagated **gradients** can be applied to tweak the subgoals ① and ② from the **failed path** to a **successful path**. One can easily plug these gradients into our algorithm.

Distance Functions (SDF) [46], enabling us to handle more complex and difficult-to-specify constraints. An example of this can be found in the simulated drone demos on our website, where we used a Neural SDF P_{duck} to model the duck obstacle in the environment. If a planned subgoal g_t is inside the obstacle, $P_{duck}(g_t)$ returns a negative value, which is false under STL semantics. To ensure that all planned subgoals stay outside the obstacle, we added an STL constraint, $\bigwedge \square_{[0,T]} P_{duck}(g_t)$, to the drone task constraints and seamlessly plugged them into our algorithm.

VI. CONCLUSIONS

Learning under formal task constraints is an important topic in robot learning. In this study, we examine the task constraints expressed in signal temporal logic. Previous research in this direction relied heavily on reward shaping and converting the constraints into sample-based policy gradients. However, we show that a more efficient approach to constraining policy searches is to backpropagate through the STL constraints, rather than reward shaping. Our results also demonstrate that our hierarchical policies can be co-optimized under these constraints, leading to improved performance compared to learning them independently.

REFERENCES

- [1] J. Fu and U. Topcu, “Probably approximately correct mdp learning and control with temporal logic constraints,” *arXiv preprint arXiv:1404.7073*, 2014.

- [2] X. Li, C.-I. Vasile, and C. Belta, "Reinforcement learning with temporal logic rewards," in *2017 IEEE/RSJ International Conference on Intelligent Robots and Systems (IROS)*. IEEE, 2017, pp. 3834–3839.
- [3] M. Hasanbeig, Y. Kantaros, A. Abate, D. Kroening, G. J. Pappas, and I. Lee, "Reinforcement learning for temporal logic control synthesis with probabilistic satisfaction guarantees," in *2019 IEEE 58th Conference on Decision and Control (CDC)*. IEEE, 2019, pp. 5338–5343.
- [4] M. Hasanbeig, D. Kroening, and A. Abate, "LCRL: Certified policy synthesis via logically-constrained reinforcement learning," in *International Conference on Quantitative Evaluation of Systems*. Springer, 2022.
- [5] K. Jothimurugan, R. Alur, and O. Bastani, "A composable specification language for reinforcement learning tasks," *Advances in Neural Information Processing Systems*, vol. 32, 2019.
- [6] Y. Jiang, S. Bharadwaj, B. Wu, R. Shah, U. Topcu, and P. Stone, "Temporal-logic-based reward shaping for continuing learning tasks," *arXiv preprint arXiv:2007.01498*, 2020.
- [7] A. K. Bozkurt, Y. Wang, M. M. Zavlanos, and M. Pajic, "Control synthesis from linear temporal logic specifications using model-free reinforcement learning," in *2020 IEEE International Conference on Robotics and Automation (ICRA)*. IEEE, 2020, pp. 10 349–10 355.
- [8] Z. Xu, I. Gavran, Y. Ahmad, R. Majumdar, D. Neider, U. Topcu, and B. Wu, "Joint inference of reward machines and policies for reinforcement learning," *Proceedings of the International Conference on Automated Planning and Scheduling*, vol. 30, no. 1, pp. 590–598, Jun. 2020.
- [9] R. T. Icarte, T. Q. Klassen, R. Valenzano, and S. A. McIlraith, "Reward machines: Exploiting reward function structure in reinforcement learning," *Journal of Artificial Intelligence Research*, vol. 73, pp. 173–208, 2022.
- [10] H. Zhang and Z. Kan, "Temporal logic guided meta q-learning of multiple tasks," *IEEE Robotics and Automation Letters*, vol. 7, no. 3, pp. 8194–8201, 2022.
- [11] C. Voloshin, H. M. Le, S. Chaudhuri, and Y. Yue, "Policy optimization with linear temporal logic constraints," *arXiv preprint arXiv:2206.09546*, 2022.
- [12] O. Maler and D. Nickovic, "Monitoring temporal properties of continuous signals," in *Formal Techniques, Modelling and Analysis of Timed and Fault-Tolerant Systems*. Springer, 2004, pp. 152–166.
- [13] K. Leung, N. Aréchiga, and M. Pavone, "Backpropagation through signal temporal logic specifications: Infusing logical structure into gradient-based methods," *Int. Journal of Robotics Research*, 2022.
- [14] K. Leung, N. Aréchiga, and M. Pavone, "Back-propagation through signal temporal logic specifications: Infusing logical structure into gradient-based methods," in *International Workshop on the Algorithmic Foundations of Robotics*. Springer, 2020, pp. 432–449.
- [15] J. Schulman, S. Levine, P. Abbeel, M. Jordan, and P. Moritz, "Trust region policy optimization," in *International conference on machine learning*. PMLR, 2015, pp. 1889–1897.
- [16] J. Schulman, F. Wolski, P. Dhariwal, A. Radford, and O. Klimov, "Proximal policy optimization algorithms," *arXiv preprint arXiv:1707.06347*, 2017.
- [17] J. Achiam, D. Held, A. Tamar, and P. Abbeel, "Constrained policy optimization," in *International conference on machine learning*. PMLR, 2017, pp. 22–31.
- [18] A. Stooke, J. Achiam, and P. Abbeel, "Responsive safety in reinforcement learning by pid lagrangian methods," in *International Conference on Machine Learning*. PMLR, 2020, pp. 9133–9143.
- [19] R. S. Sutton, D. Precup, and S. Singh, "Between mdps and semi-mdps: A framework for temporal abstraction in reinforcement learning," *Artificial intelligence*, vol. 112, no. 1-2, pp. 181–211, 1999.
- [20] O. Nachum, S. S. Gu, H. Lee, and S. Levine, "Data-efficient hierarchical reinforcement learning," *Advances in neural information processing systems*, vol. 31, 2018.
- [21] K. Jothimurugan, S. Bansal, O. Bastani, and R. Alur, "Compositional reinforcement learning from logical specifications," *Advances in Neural Information Processing Systems*, vol. 34, pp. 10 026–10 039, 2021.
- [22] Z. Xiong, J. Eappen, A. H. Qureshi, and S. Jagannathan, "Model-free neural lyapunov control for safe robot navigation," in *2022 IEEE/RSJ International Conference on Intelligent Robots and Systems (IROS)*, 2022, pp. 5572–5579.
- [23] S. Chaudhuri, K. Ellis, O. Polozov, R. Singh, A. Solar-Lezama, and Y. Yue, "Neurosymbolic programming," *Found. Trends Program. Lang.*, vol. 7, no. 3, pp. 158–243, 2021.
- [24] A. Pnueli, "The temporal logic of programs," in *18th Annual Symposium on Foundations of Computer Science (sfcs 1977)*, 1977, pp. 46–57.
- [25] G. E. Fainekos, H. Kress-Gazit, and G. J. Pappas, "Temporal logic motion planning for mobile robots," in *Proceedings of the 2005 IEEE International Conference on Robotics and Automation*. IEEE, 2005, pp. 2020–2025.
- [26] M. Kloetzer and C. Belta, "A fully automated framework for control of linear systems from temporal logic specifications," *IEEE Transactions on Automatic Control*, vol. 53, no. 1, pp. 287–297, 2008.
- [27] H. Kress-Gazit, G. E. Fainekos, and G. J. Pappas, "Temporal-logic-based reactive mission and motion planning," *IEEE Transactions on Robotics*, vol. 25, no. 6, pp. 1370–1381, 2009.
- [28] T. Wongpiromsarn, U. Topcu, and R. M. Murray, "Receding horizon temporal logic planning," *IEEE Transactions on Automatic Control*, vol. 57, no. 11, pp. 2817–2830, 2012.
- [29] C. Yang, M. L. Littman, and M. Carbin, "On the (in)tractability of reinforcement learning for LTL objectives," in *Proceedings of the Thirty-First International Joint Conference on Artificial Intelligence, IJCAI 2022*, 2022, pp. 3650–3658.
- [30] D. Andre and S. J. Russell, "State abstraction for programmable reinforcement learning agents," in *AAAI/ IAAI*, 2002, pp. 119–125.
- [31] Y. Yang, J. P. Inala, O. Bastani, Y. Pu, A. Solar-Lezama, and M. Rinarnd, "Program synthesis guided reinforcement learning for partially observed environments," in *Advances in Neural Information Processing Systems*, M. Ranzato, A. Beygelzimer, Y. Dauphin, P. Liang, and J. W. Vaughan, Eds., vol. 34. Curran Associates, Inc., 2021, pp. 29 669–29 683.
- [32] W. Qiu and H. Zhu, "Programmatic reinforcement learning without oracles," in *International Conference on Learning Representations*, 2021.
- [33] N. Ratliff, M. Zucker, J. A. Bagnell, and S. Srinivasa, "Chomp: Gradient optimization techniques for efficient motion planning," in *2009 IEEE International Conference on Robotics and Automation*. IEEE, 2009, pp. 489–494.
- [34] M. Campana, F. Lamiroux, and J.-P. Laumond, "A gradient-based path optimization method for motion planning," *Advanced Robotics*, vol. 30, no. 17-18, pp. 1126–1144, 2016.
- [35] C. Dawson and C. Fan, "Robust counterexample-guided optimization for planning from differentiable temporal logic," *arXiv preprint arXiv:2203.02038*, 2022.
- [36] A. H. Qureshi, A. Simeonov, M. J. Bency, and M. C. Yip, "Motion planning networks," in *2019 International Conference on Robotics and Automation (ICRA)*. IEEE, 2019, pp. 2118–2124.
- [37] K. He, X. Zhang, S. Ren, and J. Sun, "Deep residual learning for image recognition," in *Proceedings of the IEEE conference on computer vision and pattern recognition*, 2016, pp. 770–778.
- [38] R. T. Chen, Y. Rubanova, J. Bettencourt, and D. K. Duvenaud, "Neural ordinary differential equations," *Advances in neural information processing systems*, vol. 31, 2018.
- [39] D. P. Kingma and M. Welling, "Auto-encoding variational bayes," *arXiv preprint arXiv:1312.6114*, 2013.
- [40] T. Schaul, D. Horgan, K. Gregor, and D. Silver, "Universal value function approximators," in *International conference on machine learning*. PMLR, 2015, pp. 1312–1320.
- [41] A. Levy, R. Platt, and K. Saenko, "Hierarchical actor-critic," *arXiv preprint arXiv:1712.00948*, vol. 12, 2017.
- [42] A. Ray, J. Achiam, and D. Amodei, "Benchmarking Safe Exploration in Deep Reinforcement Learning," 2019.
- [43] E. Coumans and Y. Bai, "Pybullet, a python module for physics simulation for games, robotics and machine learning," <http://pybullet.org>, 2016–2021.
- [44] J. Panerati, H. Zheng, S. Zhou, J. Xu, A. Prorok, and A. P. Schoellig, "Learning to fly—a gym environment with pybullet physics for reinforcement learning of multi-agent quadcopter control," in *2021 IEEE/RSJ International Conference on Intelligent Robots and Systems (IROS)*, 2021.
- [45] Y. Gilpin, V. Kurtz, and H. Lin, "A smooth robustness measure of signal temporal logic for symbolic control," *IEEE Control Systems Letters*, vol. 5, no. 1, pp. 241–246, 2021.
- [46] T. Takikawa, J. Litalien, K. Yin, K. Kreis, C. Loop, D. Nowrouzezahrai, A. Jacobson, M. McGuire, and S. Fidler, "Neural geometric level of detail: Real-time rendering with implicit 3d shapes," in *Proceedings of the IEEE/CVF Conference on Computer Vision and Pattern Recognition*, 2021, pp. 11 358–11 367.